American Journal of Astronomy and Astrophysics
2025, Vol. 12, No. 1, pp. 1-8
https://doi.org/10.11648/j.ajaa.20251201.11

Research Article

Equilibrium Positions in a Gravitational Field Generated by an Elongated Asteroid with Density of Order 4

El Haj El Ourabi*, Mohammed Bennai

Quantum Physics and Magnetism Team Laboratory of Condensed Matter Physics, Faculty of Science Ben M'sik, Hassan II University, Casablanca, Morroco

Abstract

Calculating the gravitational potential generated by non-spherical mass distributions is an old problem that has been tackled by astronomical researchers. The majority of small celestial objects have an elongated shape with a non-uniform mass distribution. Early work in this field modelled these elongated bodies as segments with a uniform mass distribution. In a previous work, we established the analytical form of the potential generated by an asteroid modelled by a linear and inhomogeneous repair whose mass density is a polynomial of order four. We have studied the dynamic behavior of a test particle in the vicinity of this asteroid, which is assumed to be at rest, and have extracted periodic orbits under certain conditions. Every celestial object has an angular momentum due to its own rotation. This result in competition between gravitational attraction and centrifugal repulsion in the synodic reference frame linked to the object. This led us to focus our research on the existence of relative equilibrium positions. We calculated the Jacobi integral analytically and used the zero velocity curves numerically to extract four equilibrium positions, two isosceles and two equilateral.

Keywords

Equilibrium, Integral Jacobi, Zero Speed, Synodic

1. Introduction

Numerous studies have been carried out into the modelling of irregular bodies and the determination of the gravitational potential they generate. This approach makes it possible to analyse the equilibrium and stability of particles in the vicinity of these bodies, which is of crucial importance in the context of space missions aimed at exploring the small bodies of the solar system. Among these irregular celestial bodies, the asteroid belt offers a particularly rich field of study. These asteroids include elongated objects, and several attempts have been made to model these structures using linear mass distributions. Attempts have been made to calculate the potential generated by various geometric shapes. Werner and Scheeres treated the case of a polyhedron for asteroid 4769 Castalia [8, 9]. The case of two intersecting segments, ellipsoids and point shapes were used by Bartczak and Breiter in [10] and Bartczak et al [11] to model elongated shapes. Najid N, Zegoumou M, El ourabi E [12] modelled one of Saturn's rings by an anisotropic circular ring. Riaguas A, Elipe A and Lara M calculated the potential generated by a homogeneous segment [1]. Elipe A and Lara M studied the dynamics in the vicinity of the asteroid Eros-433 using the results of [2, 3]. Ellipe and Lara [4]

*Corresponding author: elourabis8@gmail.com (El Haj El Ourabi)

Received: 26 November 2024; **Accepted:** 10 December 2024; **Published:** 7 January 2025

described the motion around asteroid 433 Eros using the same homogeneous model. Our team Najid et al [5] proposed for the first time a new inhomogeneous parabolic density model of a static elongated body and we established the closed and analytical formula of the potential generated by this body. Following Najid and El ourabi [6], we focused on the dynamic case of the parabolic profile, concentrating on equilibrium positions and their stabilities. The effect of a higher order on the dynamic orbits was carried out by El ourabi and Bennai [7], treating the case of a polynomial profile mass density of order 4 in the static case. Our work consists of treating the case where the linear mass distribution whose generalized profile [7] is rotating around the axis of greatest moment of inertia. First, we establish the dynamic equations, in the synodic reference frame, of a test particle gravitating in the vicinity of the elongated body. In the second part we establish the algebraic equations giving the equilibrium positions in the synodic reference frame. In the last part, we carry out the energy study by calculating the Jacobi first integral, which we solve numerically using the zero velocity curves to show the existence of four equilibrium positions.

2. Dynamical Study

2.1. Potential Gravitational

The elongated body, of mass M and length $2l$, is modelled by a segment centred at O, Figure 1 and Figure 2 Non-homogeneity is characterised by the density:

$$\lambda(x) = b - ax^2 + cx^4 \quad (1)$$

The mass of the body is:

$$M = 2bl - \frac{2}{3}al^3 + \frac{2}{5}cl^5$$

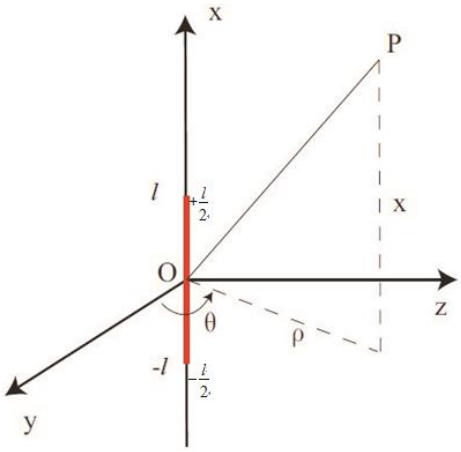

Figure 1. *Study coordinates (ρ,θ,x).*

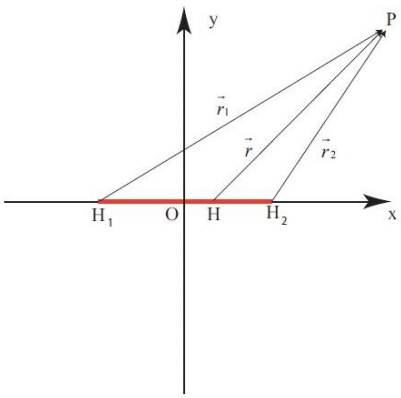

Figure 2. *Coordinates r_1 and r_2.*

The analytical expression of the gravitational potential is given in [7]:

$$U(P) = -G\left[z_1 + \frac{r_1}{2l}z_2 + \frac{r_2}{2l}z_3 + z_4 Ln\left(\frac{s+2l}{s-2l}\right)\right] \quad (2)$$

with G the Cavendish constant. The coefficients $(z_i)_{i=1..4}$ depend on the position of the point P, their expressions are:

$$z_1 = -\frac{55}{48}a_4BC^{\frac{3}{2}} + \frac{2}{3}a_3BC^{\frac{3}{2}}$$

$$z_2 = \frac{35}{64}a_4B^3 - \frac{5}{8}a_3B^2 + \frac{3}{4}a_2B - a_1$$

$$z_3 = -\frac{35}{64}a_4B^3 + \left(\frac{35}{96}a_4 + \frac{5}{8}a_3\right)B^2 - \left(\frac{5}{12}a_3 + \frac{7}{24}a_4 + \frac{3}{4}a_2\right)B + \frac{55}{48}a_4BC$$

$$-\left(\frac{3}{8}a_4 + \frac{2}{3}a_3\right)C + a_1 + \frac{1}{2}a_2 + \frac{1}{3}a_3 + \frac{1}{4}a_4$$

$$z_4 = \frac{35}{128}a_4B^4 - \frac{5}{16}a_3B^3 - \frac{15}{16}a_4CB^2 + \frac{3}{8}a_2B^2 + \frac{3}{4}CB - \frac{1}{2}a_1B + \frac{3}{8}a_4C^2 - \frac{1}{2}a_2C + a_0$$

s, B and C are functions of the position of point P, they are given by:

$$s = r_1 + r2,\ r_1 = \sqrt{(x+l)^2 + y^2 + z^2},\ r_2 = \sqrt{(x-l)^2 + y^2 + z^2}$$

$$B = \frac{r_2^2 - r_1^2 - 4l^2}{4l^2} \quad ; \quad C = \frac{r_1^2}{4l^2}$$

a_0, a_1, a_2, a_3 and a_4 are the constants given by:

$$a_0 = b - al^2 + cl^4,\ a_1 = 4l^2(a - cl^2),\ a_2 = 4l^2(5cl^2 - a),\ a_3 = -32cl^4,\ a_4 = 16cl^4$$

2.2. Equations of Motion

The speed of rotation of the body relative to (OZ) is de-

noted by ω and the test particle is placed at point P as shown in Figure 3.

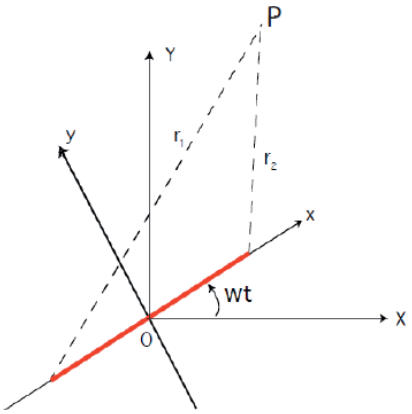

Figure 3. *Synodical reference.*

The dynamic equation in the synodic reference frame R is:

$$\left(\frac{d^2\overrightarrow{OP}}{dt^2}\right)_R + 2\vec{\omega} \wedge \left(\frac{d\overrightarrow{OP}}{dt}\right)_R + \vec{\omega} \wedge \left(\vec{\omega} \wedge \overrightarrow{OP}\right) = -\overleftarrow{\nabla} U(P) \quad (3)$$

By injecting expression (2) into equation (3) and projecting into the synodic reference frame we obtain:

$$\ddot{x} - 2\omega\dot{y} = \omega^2 x - \frac{\partial U}{\partial x} \quad (4)$$

$$\ddot{y} + 2\omega\dot{x} = \omega^2 y - \frac{\partial U}{\partial y} \quad (5)$$

$$\ddot{z} = -\frac{\partial U}{\partial z} \quad (6)$$

The effective potential W is given by the contribution of the gravitational potential and the centrifugal potential:

$$W(x,y,z) = U(P) - \frac{\omega^2}{2}(x^2 + y^2)$$

The equations (4, 5, 6) give:

$$\ddot{x} - 2\omega\dot{y} = -W_x \quad (7)$$

$$\ddot{y} + 2\omega\dot{x} = -W_y \quad (8)$$

$$\ddot{z} = -W_z \quad (9)$$

With $W_x = \frac{\partial W}{\partial x}$. $W_y = \frac{\partial W}{\partial y}$, and $W_z = \frac{\partial W}{\partial z}$ Their expressions are:

$$\begin{aligned} Wx \quad = & -G\left(\left(\frac{2}{3}a_3 - \frac{55}{48}\right)\left(\frac{d^2-s^2}{4lp}C^{3/2} + 3\frac{x+l}{4l^2}C^{1/2}B\right)\right. \\ & + \frac{r_1}{2l}\frac{d^2-s^2}{4lp}\left(\frac{105}{64}a_4B^2 - \frac{5}{4}a_3B + \frac{3}{4}a_2\right) \\ & + z_2\frac{x+l}{2r_1l} \\ & + \frac{r_2}{2l}\left(\left[-\frac{99}{64}a_4B^2 + 2\left(\frac{35}{96}a_4 + \frac{5}{8}a_3\right)B - \left(\frac{5}{12}a_3 + \frac{7}{24}a_4 + \frac{3}{4}a_2\right)\right]\frac{d^2-s^2}{4lp}\right. \\ & - \frac{55}{48}a_4\left(\frac{d^2-s^2}{4lp}C + \frac{x+l}{2l^2}B\right) - \left(\frac{3}{4}a_4 + \frac{2}{3}a_3\right)\frac{x+l}{2l^2} \\ & + \frac{x-l}{2lr_2}z_3 \\ & + \left[\left(\frac{35}{32}a_4B^3 - \frac{15}{16}a_3B^2 + \frac{3}{4}a_2B - \frac{a_1}{2}\right)\frac{d^2-s^2}{4lp}\right. \\ & - \frac{15}{16}\left(2BC\frac{d^2-s^2}{4lp} + B^2\frac{x+l}{2l^2}\right) \\ & + \frac{3}{4}\left(B\frac{x+l}{2l^2} + C\frac{d^2-s^2}{4lp}\right) \\ & \left. + \left(\frac{3}{4}a_4C - \frac{a_2}{2}\right)\frac{x+l}{2l^2}\right]\ln\left(\frac{s+2l}{s-2l}\right) \\ & \left. - \frac{4l(sx-ld)}{p(s^2-4l^2)}z_4\right) - \omega^2 x \end{aligned} \quad (10)$$

$$\begin{aligned} W_y \quad = & -G\left\{\left(\frac{2a_3}{3} - \frac{55a_4}{48}\right)\frac{3y}{4l^2}BC^{1/2} + \frac{z_2y}{2lr_1} + \frac{r_2}{2l}\left(-\frac{55a_4yB}{96l^2} - \left(\frac{3a_4}{8} + \frac{2a_3}{3}\right)\frac{y}{2l^2}\right)\right. \\ & + \frac{yz_3}{2lr_2} + \left(-\frac{15a_4B^2}{16} + \frac{3B}{4} + \frac{3a_4C}{4} - \frac{a_2}{2}\right)\frac{y}{2l^2}\ln\left(\frac{s+2l}{s-2l}\right) \\ & \left. - \frac{4yslz_4}{p(s^2-4l^2)}\right\} - \omega^2 y \end{aligned} \quad (11)$$

$$W_z = -G\left\{\left(\frac{2a_3}{3}-\frac{55a_4}{48}\right)\frac{3zBC^{1/2}}{4l^2}+\frac{zz_2}{2lr_1}+\frac{r_2}{2l}\left(-\frac{55a_4zB}{96l^2}-\left(\frac{3a_4}{8}+\frac{2a_3}{3}\right)\frac{z}{2l^2}\right)+\left(\frac{15a_4B^2}{16}+\frac{3B}{4}+\frac{3a_4C}{4}-\frac{a_2}{2}\right)\frac{z}{2l^2}\ln\left(\frac{s+2l}{s-2l}\right)-\frac{4zslz_4}{p(s^2-4l^2)}\right\} \quad (12)$$

The dynamic equations become:

$$\begin{aligned}\ddot{x}-2\omega\dot{y} = G\Big\{&\left(\frac{2}{3}a_3-\frac{55}{48}\right)\left(\frac{d^2-s^2}{4lp}C^{3/2}+3\frac{x+l}{4l^2}C^{1/2}B\right)\\&+\frac{r_1}{2l}\frac{d^2-s^2}{4lp}\left(\frac{105}{64}a_4B^2-\frac{5}{4}a_3B+\frac{3}{4}a_2\right)\\&+z_2\frac{x+l}{2r_1l}\\&+\frac{r_2}{2l}\Bigg(\left(-\frac{99a_4B^2}{64}+2\left(\frac{35a_4}{96}+\frac{5a_3}{8}\right)B\right.\\&\left.-\left(\frac{5a_3}{12}+\frac{7a_4}{24}+\frac{3a_2}{4}\right)\right)\frac{d^2-s^2}{4lp}-\frac{55a_4}{48}\left(\frac{d^2-s^2}{4lp}C+\frac{x+l}{2l^2}B\right)\\&-\left(\frac{3a_4}{4}+\frac{2a_3}{3}\right)\frac{x+l}{2l^2}\Bigg)+\frac{x-l}{2lr_2}z_3\\&+\Bigg(\left(\frac{35a_4}{32}B^3-\frac{15a_3}{16}B^2+\frac{3a_2}{4}B-\frac{a_1}{2}\right)\frac{d^2-s^2}{4lp}\\&-\frac{15a_4}{16}\left(2BC\frac{d^2-s^2}{4lp}+B^2\frac{x+l}{2l^2}\right)\\&+\frac{3}{4}\left(B\frac{x+l}{2l^2}+C\frac{d^2-s^2}{4lp}\right)\\&+\left(\frac{3a_4}{8}C-\frac{a_2}{2}\right)\frac{x+l}{s-2l}\Bigg)Ln\left(\frac{s+2l}{s-2l}\right)\\&-\frac{4l(sx-ld)}{p(s^2-4l^2)}z_4\Big\}-\omega^2x\end{aligned} \quad (13)$$

$$\begin{aligned}\ddot{y}+2\omega\dot{x} = G\Big\{&\left(\frac{2a_3}{3}-\frac{55a_4}{48}\right)\frac{3y}{4l^2}BC^{1/2}+\frac{z_2y}{2lr_1}+\frac{r_2}{2l}\left(-\frac{55a_4yB}{96l^2}-\left(\frac{3a_4}{8}+\frac{2a_3}{3}\right)\frac{y}{2l^2}\right)\\&+\frac{yz_3}{2lr_2}+\left(-\frac{15a_4B^2}{16}+\frac{3B}{4}+\frac{3a_4C}{4}-\frac{a_2}{2}\right)\frac{y}{2l^2}\ln\left(\frac{s+2l}{s-2l}\right)\\&-\frac{4yslz_4}{p(s^2-4l^2)}\Big\}-\omega^2y\end{aligned} \quad (14)$$

$$\ddot{z} = G\left\{\left(\frac{2a_3}{3}-\frac{55a_4}{48}\right)\frac{3zBC^{1/2}}{4l^2}+\frac{zz_2}{2lr_1}+\frac{r_2}{2l}\left(-\frac{55a_4zB}{96l^2}-\left(\frac{3a_4}{8}+\frac{2a_3}{3}\right)\frac{z}{2l^2}\right)+\left(\frac{15a_4B^2}{16}+\frac{3B}{4}+\frac{3a_4C}{4}-\frac{a_2}{2}\right)\frac{z}{2l^2}\ln\left(\frac{s+2l}{s-2l}\right)-\frac{4zslz_4}{p(s^2-4l^2)}\right\} \quad (15)$$

3. The Equilibria

3.1. Equations of Equilibria

From expressions (13), (14) and (15) we derive the equations for the equilibrium positions:

$$
\begin{aligned}
&G\left\{\left(\frac{2}{3}a_3-\frac{55}{48}\right)\left(\frac{d^2-s^2}{4lp}C^{3/2}+3\frac{x+l}{4l^2}C^{1/2}B\right)\right.\\
&+\frac{r_1}{2l}\frac{d^2-s^2}{4lp}\left(\frac{105}{64}a_4B^2-\frac{5}{4}a_3B+\frac{3}{4}a_2\right)\\
&+z_2\frac{x+l}{2r_1l}\\
&+\frac{r_2}{2l}\left(\left(-\frac{99a_4B^2}{64}+2\left(\frac{35a_4}{96}+\frac{5a_3}{8}\right)B\right.\right.\\
&\left.-\left(\frac{5a_3}{12}+\frac{7a_4}{24}+\frac{3a_2}{4}\right)\right)\frac{d^2-s^2}{4lp}-\frac{55a_4}{48}\left(\frac{d^2-s^2}{4lp}C+\frac{x+l}{2l^2}B\right)\\
&\left.-\left(\frac{3a_4}{4}+\frac{2a_3}{3}\right)\frac{x+l}{2l^2}\right)+\frac{x-l}{2lr_2}z_3\\
&+\left(\left(\frac{35a_4}{32}B^3-\frac{15a_3}{16}B^2+\frac{3a_2}{4}B-\frac{a_1}{2}\right)\frac{d^2-s^2}{4lp}\right.\\
&-\frac{15a_4}{16}\left(2BC\frac{d^2-s^2}{4lp}+B^2\frac{x+l}{2l^2}\right)\\
&+\frac{3}{4}\left(B\frac{x+l}{2l^2}+C\frac{d^2-s^2}{4lp}\right)\\
&\left.+\left(\frac{3a_4}{8}C-\frac{a_2}{2}\right)\frac{x+l}{s-2l}\right)Ln\left(\frac{s+2l}{s-2l}\right)\\
&\left.-\frac{4l(sx-ld)}{p(s^2-4l^2)}z_4\right\}-\omega^2x=0
\end{aligned}
\tag{16}
$$

$$
\begin{aligned}
&G\left\{\left(\frac{2a_3}{3}-\frac{55a_4}{48}\right)\frac{3y}{4l^2}BC^{1/2}+\frac{z_2y}{2lr_1}+\frac{r_2}{2l}\left(-\frac{55a_4yB}{96l^2}-\left(\frac{3a_4}{8}+\frac{2a_3}{3}\right)\frac{y}{2l^2}\right)\right.\\
&+\frac{yz_3}{2lr_2}+\left(-\frac{15a_4B^2}{16}+\frac{3B}{4}+\frac{3a_4C}{4}-\frac{a_2}{2}\right)\frac{y}{2l^2}\ln\left(\frac{s+2l}{s-2l}\right)\\
&\left.-\frac{4yslz_4}{p(s^2-4l^2)}\right\}-\omega^2y=0
\end{aligned}
\tag{17}
$$

$$
\begin{aligned}
&G\left\{\left(\frac{2a_3}{3}-\frac{55a_4}{48}\right)\frac{3zBC^{1/2}}{4l^2}+\frac{zz_2}{2lr_1}+\frac{r_2}{2l}\left(-\frac{55a_4zB}{96l^2}-\left(\frac{3a_4}{8}+\frac{2a_3}{3}\right)\frac{z}{2l^2}\right)\right.\\
&+\left(\frac{15a_4B^2}{16}+\frac{3B}{4}+\frac{3a_4C}{4}-\frac{a_2}{2}\right)\frac{z}{2l^2}\ln\left(\frac{s+2l}{s-2l}\right)\\
&\left.-\frac{4zslz_4}{p(s^2-4l^2)}\right\}=0
\end{aligned}
\tag{18}
$$

Equation (18) shows that the equilibrium positions are contained in the (x,y) plane.

3.2. Zero Velocity Curves

The zero-velocity curves show lines separating the zones permitted and those prohibited by the test particle. See more details in [15, 16].

The dynamic system defined by equations (7), (8) and (9) has a first integral characterized by the Jacobi constant C_J related to the energy of the system. This first integral is described by:

$$C_J = 2W(x,y,z) + (\dot{x}^2 + \dot{y}^2 + \dot{z}^2)$$

For well-defined initial conditions, the orbit of the test particle must lie inside the curve of equation $2W(x, y, z) \leq C$. The zero velocity surface is expressed by the relation $C = 2W(x,y,z)$. In this case the contour delimiting the permitted zones from the forbidden zones is given by the equation

$$g(x,y,C) = 2W - C = 0$$

Figures 4, 5 and 6 show a numerical resolution of the zero velocity curves for different values of the Jacobi constant.

The curves in (Figure 4):

1) (Figure 4-a) is plotted for $l = 0.5$, $a = 0.1$, $b = 1$, $c = 0.01$, $w = 0.8$ and for the values of the Jacobi constant:

−1.1, −1.2,−1.3,−1.31,−1.32,−1.33,−1.34,−1.24,−1.25

−1.26, −1.27,−1.28,−1.29,−1.4,−1.45,−1.46,−1.47,−1.48

−1.49, −1.5,−1.6,−1.7,−1.8,−1.9,−2,−2.5,−3,−3.5

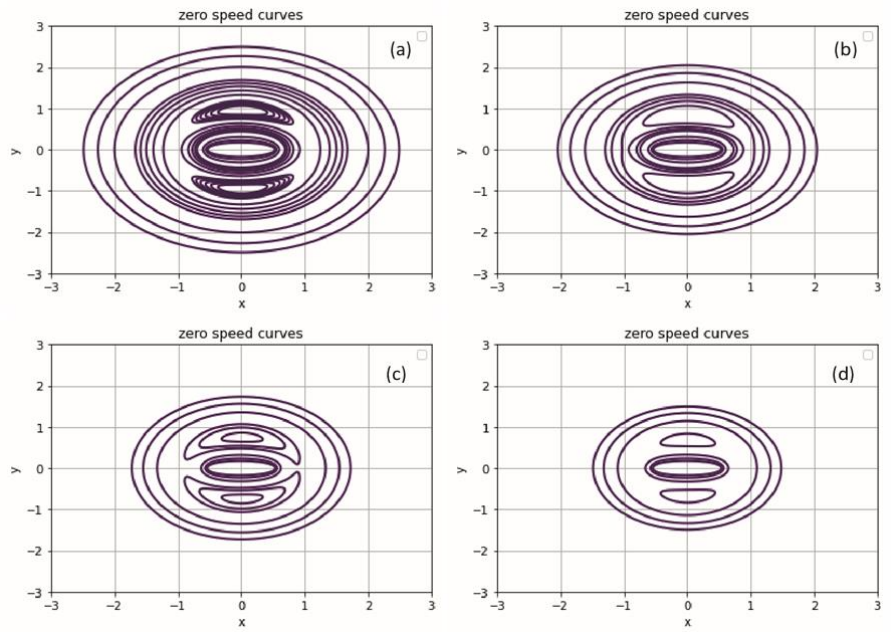

Figure 4. *Zero velocity curves.*

2) (Figure 4-b) is plotted for $l = 0.5$, $a = 0.1$, $b = 1$, $c = 0.01$, $w = 1$ and for the values of the Jacobi constant:

−1.1,−1.2,−1.3,−1.31,−1.32,−1.33,−1.34,−1.24,−1.25

−1.26,−1.27,−1.28,−1.29,−1.4,−1.45,−1.46,−1.47,−1.48

−1.49,−1.5,−1.6,−1.7,−1.8,−1.9,−2,−2.5,−3,−3.5

3) (Figure 4-c) is plotted for $l = 0.5$, $a = 0.1$, $b = 1$, $c = 0.01$, $w = 1.2$ and for the values of the Jacobi constant:

−1.1,−1.2,−1.3,−1.31,−1.32,−1.33,−1.34,−1.24,−1.25

−1.26,−1.27,−1.28,−1.29,−1.4,−1.45,−1.46,−1.47,−1.48

−1.49,−1.5,−1.6,−1.7,−1.8,−1.9,−2,−2.5,−3,−3.5

4) (Figure 4-d) is plotted for $l = 0.5$, $a = 0.1$, $b = 1$, $c = 0.05$, $w = 0.8$ and for the values of the Jacobi constant:

−1.1,−1.2,−1.3,−1.31,−1.32,−1.33,−1.34,−1.24,−1.25

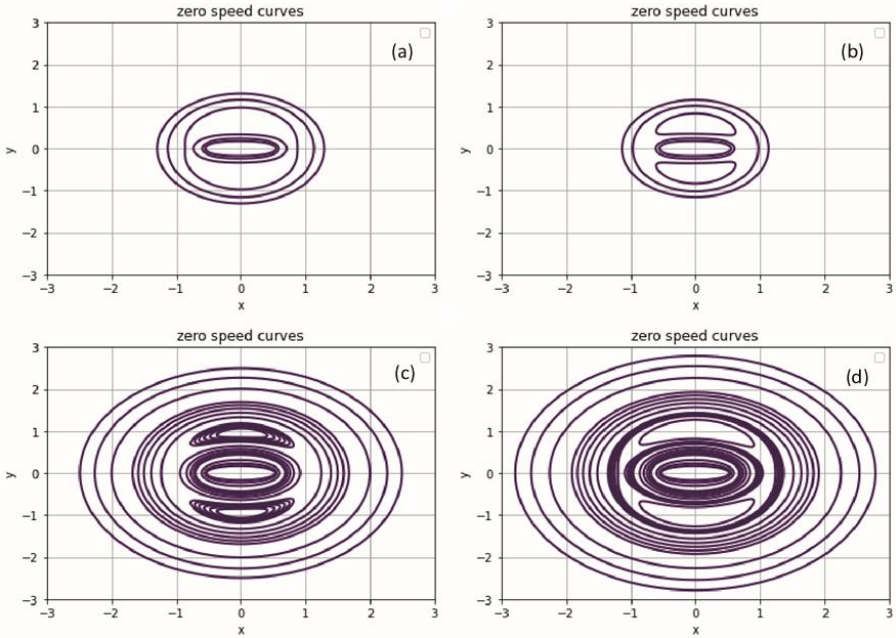

Figure 5. *Zero velocity curves.*

−1.26,−1.27,−1.28,−1.29,−1.4,−1.45,−1.46,−1.47,−1.48

−1.49,−1.5,−1.6,−1.7,−1.8,−1.9,−2,−2.5,−3,−3.5

*The curves in (*Figure 5*):*

1) (Figure 5-a) is plotted for $l = 0.5$, $a = 0.1$, $b = 1$, $c = 0.01$, $w = 0.8$ and for the values of the Jacobi constant:

−1.1,−1.2,−1.3,−1.31,−1.32,−1.33,−1.34,−1.24,−1.25

2) (Figure 5-b) is plotted for $l = 0.5$, $a = 0.1$, $b = 1$, $c = 0.02$, $w = 0.8$ and for the values of the Jacobi constant:

−1.1,−1.2,−1.3,−1.31,−1.32,−1.33,−1.34,−1.24,−1.25

3) (Figure 5-c) is plotted for $l = 0.5$, $a = 0.1$, $b = 1$, $c = 0.01$, $w = 1.4$ and for the values of the Jacobi constant:

−1.1,−1.2,−1.3,−1.31,−1.32,−1.33,−1.34,−1.24,−1.25

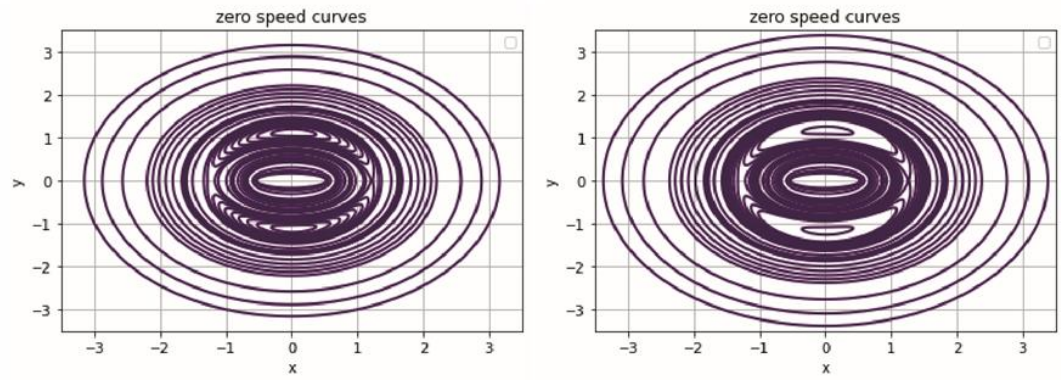

Figure 6. *Zero velocity curves.*

−1.26,−1.27,−1.28,−1.29,−1.4,−1.45,−1.46,−1.47,−1.48

−1.49,−1.5,−1.6,−1.7,−1.8,−1.9,−2,−2.5,−3,−3.5

4) (Figure 5-d) is plotted for $l = 0.5$, $a = 0.1$, $b = 1$, $c = 0.05$, $w = 2$ and for the values of the Jacobi constant:

−1.1,−1.2,−1.3,−1.31,−1.32,−1.33,−1.34,−1.24,−1.25

−1.26,−1.27,−1.28,−1.29,−1.4,−1.45,−1.46,−1.47,−1.48

−1.49,−1.5,−1.6,−1.7,−1.8,−1.9,−2,−2.5,−3,−3.5

*The curves in (*Figure 6*):*

1) (Figure 6-a) is plotted for $l = 0.5$, $a = 0.1$, $b = 1$, $c = 0.01$, $w = 2$ and for the values of the Jacobi constant:

−1.1,−1.2,−1.3,−1.31,−1.32,−1.33,−1.34,−1.24,−1.25

−1.26,−1.27,−1.28,−1.29,−1.4,−1.45,−1.46,−1.47,−1.48

−1.49,−1.5,−1.6,−1.7,−1.8,−1.9,−2,−2.5,−3,−3.5,−3.6,−3.8,−4

2) (Figure 6-b) is plotted for$l = 0.5$, $a = 0.1$, $b = 1$, $c = 0.02$, $w = 2.5$ and for the values of the Jacobi constant:

−1.1,−1.2,−1.3,−1.31,−1.32,−1.33,−1.34,−1.24,−1.25

−1.26,−1.27,−1.28,−1.29,−1.4,−1.45,−1.46,−1.47,−1.48
−1.49,−1.5,−1.6,−1.7,−1.8,−1.9,−2,−2.5,−3,−3.5,−3.6,−3.8,−4

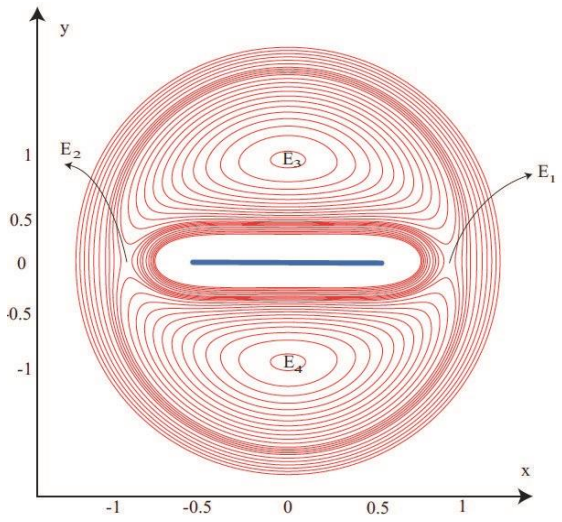

Figure 7. *Equilibrium positions.*

The zero velocity curves show that there are four equilibrium positions, (Figure 7):

Colinear positions E_1 et E_2.

Isosceles positions: E_3 et E_4.

4. Conclusion

The study we have developed models the behavior of a low-mass space probe orbiting in the gravitational field generated by an elongated asteroid, which has been modelled by an inhomogeneous linear distribution in rotation. The mass profile of the asteroid is characterized by a symmetric fourth-order polynomial density. We have established the dynamical equations of motion in the synodic reference frame associated with the irregular body, as well as those for the relative equilibrium positions. The numerical resolution of the zero-velocity curves has enabled us to find four symmetrical equilibrium positions, two of which are collinear with the segment and two of which lie on the axis orthogonal to the segment and passing through its centre. Locating the equilibrium positions saves energy and costs for space missions to explore irregular celestial bodies such as NEAR Shoemaker and ROSETTA, which have been carried out by space agencies such as ESA and NASA [13] and [14]. Our future plans include exploring the case of more detailed mass distributions, namely volume distributions.

Abbreviations

NEAR Near Earth Asteroid Rendezvous

Conflicts of Interest

The authors declare no conflicts of interest.

References

[1] Riaguas A, Elipe A, Lara M. Periodic orbits around a massive straight segment. Celest. Mech. Dyn. Astron. 1999; 73(1-4): 169-78. https://doi.org/10.1023/A:1008399030624

[2] Elipe A, Lara M. A simple model for the chaotic motion around (433) Eros. J. astronaut. sci. 2003; 51: 391-404. https://doi.org/10.1007/BF03546290

[3] Elipe A, Lara M. A simple model for the chaotic motion around (433) Eros. Adv. Astronaut. Sci. 2004; 116: 1-5. https://doi.org/10.1007/BF03546290

[4] Ellipe, A. and Lara, M. 2003, The Journal of Astronautical Sciences, 51, 391.

[5] Najid NE, Zegoumou M. Potential generated by a massive inhomogeneous straightsegment. Res. Astron. Astrophys. 2011; 11(3): 345. https://doi.org/10.1088/1674-4527/11/3/008

[6] Najid NE, El Elourabi H. Equilibria and stability around a straight rotating segment with a parabolic profile of mass density. Open Astron. J. 2012; 5(1). https://doi.org/10.2174/1874381101205010019

[7] El haj El ourabi, Mohamed Bennai. Modelling the Dynamics of a Probe in Vicinityof Eross-433 With a Fourth-Order Polynomial Density Profile, 29 June 2023. Journal of Physics and Astronomy. Vol 11, Iss 8. https://doi.org/10.21203/rs.3.rs-3107459/v1

[8] Werner RA. The gravitational potential of a homogeneous polyhedron or don't cutcorners. Celest. Mech. Dyn. Astron. 1994; 59: 253-78. https://doi.org/10.1007/BF006928759

[9] Werner RA, Scheeres DJ. Exterior gravitation of a polyhedron derived and compared with harmonic and mascon gravitation representations of asteroid 4769 Castalia. Celest. Mech. Dyn. Astron. 1996; 65: 313-44. https://doi.org/10.1007/BF00053511

[10] Bartczak P, Breiter S. Double material segment as the model of irregular bodies. Celest. Mech. Dyn. Astron. 2003; 86(2): 131-41. https://doi.org/10.1023/A:1024115015470

[11] Bartczak P, Breiter S, Jusiel P. Ellipsoids, material points and material segments. Celest. Mech. Dyn. Astron. 2006; 96: 31-48. https://doi.org/10.1007/s10569-006-9017-x

[12] Najid NE, Zegoumou M, El Elourabi H. Dynamical behavior in the vicinity of acircular anisotropic ring. Open Astron. J. 2012; 5(1). https://doi.org/10.1007/s11071-015-2322-8

[13] NEAR. Special Issue on the NEAR Mission to 433 Eros. J Astronaut Sci 1995; 43: 477. https://doi.org/10.1029/96JE03364

[14] Schwehm G, Hechler M. Rosetta -ESA's planetary cornestone mission. ESA Bull1994; 77: 7-18.

[15] Pal, A. K., Abouelmagd, E. I., Kishor, R. Effect of Moon perturbation on theenergy curves and equilibrium points in the Sun–Earth–Moon system. New Astronomy, 2021; 84, 101505. https://doi.org/10.1016/j.nevast.2020.101505

[16] Zotos, E. E., Abouelmagd, E. I., Abd El Motelp, N. S. Introducing a new version of the restricted three-body problem with a continuation fraction potential. New. Astronomy, 2020; 81, 101444. https://doi.org/10.1016/j.nevast.2020.101444